

Lawrence Berkeley National Laboratory

Lawrence Berkeley National Laboratory

Title

Bonding in Copper (II) Chelates: Solvent Effects in their Visible Absorption

Permalink

<https://escholarship.org/uc/item/7sm968hm>

Authors

Belford, R. Linn
Calvin, M.
Belford, Geneva

Publication Date

1956-09-01

UNIVERSITY OF
CALIFORNIA

*Radiation
Laboratory*

BONDING IN COPPER (II) CHELATES:
SOLVENT EFFECTS IN THEIR VISIBLE
ABSORPTION SPECTRA

TWO-WEEK LOAN COPY

*This is a Library Circulating Copy
which may be borrowed for two weeks.
For a personal retention copy, call
Tech. Info. Division, Ext. 5545*

UNIVERSITY OF CALIFORNIA

Radiation Laboratory
Berkeley, California

Contract No. W-7405-eng -48

BONDING IN COPPER (II) CHELATES:
SOLVENT EFFECTS IN THEIR VISIBLE ABSORPTION SPECTRA

R. Lim Belford, M. Calvin, and Geneva Belford

September 1956

BONDING IN COPPER (II) CHELATES:
SOLVENT EFFECTS IN THEIR VISIBLE ABSORPTION SPECTRA

Contents

Abstract	3
Introduction	4
Experimental	6
Preparation of Materials	6
Results and Discussion	7
Identification of Transitions	11
Predictions from Crystal-Field Theory	15
Allowance for Covalency	17
MO Predictions	20
Appendix	
Molecular (Crystal) Field Treatment	22
Special Case of Point-Charge Ligands	22
General Case	25
Molecular Orbital Treatment	28

BONDING IN COPPER (II) CHELATES:
SOLVENT EFFECTS IN THEIR VISIBLE ABSORPTION SPECTRA

R. Linn Belford^{*,†}, M. Calvin, and Geneva Belford^{**}

Radiation Laboratory and Department of Chemistry
University of California, Berkeley, California

September 1956

ABSTRACT

Absorption spectra, in the visible red and near infrared, are reported for solutions of bis-acetylacetonate-Cu(II) and its 3-ethyl variant in various media. The spectra could arise from a set of three Gaussian components whose positions and intensities are shown to depend primarily upon solvent basicity. These component bands are identified with three $3d^1-3d^1$ transitions predicted from crystal field and molecular orbital theories. The behavior of these bands upon alteration of solvent and of chelate ring substituents appears consistent with the postulate that pi-bonding changes are energetically of less importance than changes in crystal field splitting and in sigma bonding.

* National Science Foundation Predoctoral Fellow, 1954-55.

† Present address, Department of Chemistry, University of Illinois, Urbana, Illinois.

** Genevieve McEnerney Predoctoral Fellow in Mathematics, 1954-55.

BONDING IN COPPER (II) CHELATES:
SOLVENT EFFECTS IN THEIR VISIBLE ABSORPTION SPECTRA

R. Linn Belford, M. Calvin, and Geneva Belford
Radiation Laboratory and Department of Chemistry
University of California, Berkeley, California

September 1956

INTRODUCTION

The detailed electronic structures--that is to say, the nature of the bonds--in most of the chelate compounds of transition metal ions are still undertermined. It has been the practice of many workers in the field, therefore, to assume one or another extreme picture for bonding--e. g., completely covalent or completely ionic--and to ignore totally the other viewpoints. On the other hand, some of us have chosen to accept often flimsy criteria to classify a particular chelate either as covalent or as ionic. That these criteria provide no distinction at all is easily demonstrated. The solubility of a complex in organic solvents, for instance, is extensively regarded as evidence of the covalent bond type. However, it is in reality only evidence that there are no strong intermolecular ionic forces in the chelate. For example, to dissolve sodium chloride as NaCl molecules one must break five nearest-neighbor $\text{Na}^+ \text{Cl}^-$ lattice bonds; to dissolve cobalt(III) tris-acetylacetonate, regardless of its bond type, one need only overcome Van der Waals attraction between virtual hydrocarbons. Only for those (comparatively few) anions which would surely bridge two or more metal ions if covalency were not important can solubility in organic solvents furnish a clue as to the nature of the bonds. Likewise, the magnetic criterion for bond type, so confidently invoked by nearly all coordination chemists until recently, has been shown by Orgel¹ to be invalid. It is true that the magnetic susceptibility of certain complexes may still allow one to rule out extreme covalent pictures, as in the paramagnetic nickel(II) chelates, but it does not exclude appreciable covalent character nor does it ever forbid an ionic picture.

¹ L. E. Orgel, J. Chem. Soc. 1952, 4756.

Because of the failure of the older criteria to furnish sufficient information regarding the nature of bonding in metal-organic chelates, we have thought it worth while to investigate some different methods. It is valuable to have a more intimate picture of the magnetic behavior of the unpaired electron than that furnished by the bulk magnetic susceptibility. Dr. B. R. McGarvey's work on the paramagnetic resonance of Cu(II) acetylacetonate is beginning to supply this aspect.² This paper is concerned with visible and near-infrared absorption spectra.

Recently a number of other workers have shown interest in the visible and near-infrared absorption of the transition metal ions, particularly as the spectra are influenced by, or arise from, the so-called crystalline electric field of the surrounding dipolar molecules. Orgel¹ has discussed the application of the crystal field theory to complexes of these atoms in a general way, and has proposed that the ionic viewpoint thus adopted is capable of explaining most of their properties, e. g., magnetic susceptibility and spectra. Hartmann, Ilse, and Schlafer^{3, 4, 5, 6} have applied the crystal field theory to the electronic spectrum of $Ti^{+++}.6H_2O$ and of some V^{+++} complexes with some success. Ballhausen⁷ and Bjerrum, Ballhausen, and Jørgensen⁸ have attempted to calculate the absorption spectra of complexes of Cu(II) with water and with ammonia; they consider the results quantitatively meaningful and attach significance to discrepancies between the observed spectra and their calculations for certain models. Holmes and McClure⁹ have studied the absorption spectra of single crystals of transition metal ion hydrates and have been quite successful in explaining the experiments in terms of the crystal field theory; their assumptions are fewer than those

² B. R. McGarvey, J. Phys. Chem. 60, 71 (1956).

³ F. E. Ilse and H. Hartmann, Z. Naturforsch. 6a, 751 (1951).

⁴ F. E. Ilse and H. Hartmann, Z. Physik. Chem. 197, 239 (1951).

⁵ H. Hartmann and H. L. Schlafer, Z. Naturforsch. 6a, 754 (1951).

⁶ Ibid., p. 760

⁷ C. J. Ballhausen, Dan. Mat. Fys. Medd. 29, No. 4, (1954).

⁸ Bjerrum, Ballhausen, and Jørgensen, Acta Chem. Scand. 8, 1275 (1954).

⁹ O. Holmes, Ph.D. thesis, University of California, 1955.

of the Danish authors.^{7,8} They have not attempted to obtain absolute numerical values from the calculations, but have treated every quantity not determined by the symmetry of the model alone as an undetermined parameter, to be fixed by experiment.

We have chosen the Cu(II) chelate of acetylacetonone for study because it is stable and easy to prepare, because it is one of very few metallo-organic chelates whose complete x-ray structure has been worked out,¹⁰ because it has higher symmetry than most of the available compounds, and because its red absorption bands are not obscured by tail-off from the strong blue and ultraviolet absorption.

EXPERIMENTAL

The visible and near infrared absorption spectra of Cu(II) bis-acetylacetonone (CuA_2) and Cu(II) bis-3-ethylacetylacetonone (CuEa_2) were measured with a Beckman DK recording spectrophotometer. The lead sulfide detector was always used through the whole range of the measurements; small slit widths were maintained. Scanning was at medium or slow speed. Wave lengths were marked on each spectrum by tapping a microswitch which shorted the sample circuit; the technique gives the same result as flicking the shutter on the sample beam, but allows better precision. Immediately prior to each spectral run, a base line was run on the same chart with pure solvent in both cells.

Preparation of Materials

The solutes employed were freshly recrystallized from toluene and were desiccated. Sources of the spectroscopic solvents were as follows: Chloroform was Merck reagent grade; nitrobenzene was supplied by Eastman and was distilled at aspirator pressure, bp $89.2 \pm 0.5^\circ\text{C}$; benzene, acetone, and pyridine were Baker and Adamson reagent grade; 1,4-dioxane was Eastman and was purified by low-pressure distillation; methanol was Eastman spectro grade, No. S 467; n-pentanol was Merck reagent grade, dried with calcium sulfate and distilled after refluxing with similarly dried Eastman white label n-amyl n-butyrate plus Na pieces.

¹⁰ Koyama, Saito, and Kuroya, J. Inst. Polytechnics, Osaka City University C4, 43 (1953).

Table I

Component absorption bands of Cu(II) bis-acetylacetonone in the visible and near infrared ^a									
Solvent ^b	ω_1^0	$\epsilon_{1\max}$	$1\delta_{1/2}$	ω_2^0	$\epsilon_{2\max}$	$2\delta_{1/2}$	ω_s^0	$\epsilon_{3\max}$	$3\delta_{1/2}$
I Chloroform ^c	18810	26.3	1910	15190	(34.1)	1690	--	--	--
II 1,4-Dioxane ^c	17500	32	1750	15100	22	1700	13500	11	1600
III n-Pentanol ^d	17100	28	2300	15200	24	1800	13000	13	1750
IV Pyridine ^c	15900	42.5	1750	14800	28	1900	12100	26	2330
V Piperidine ^c	15100	45	2200	14800	32	1800	11300	43	2300

^a All frequencies and half widths given in Cm^{-1} . $i\delta_{1/2}$ = half width at $\epsilon = \epsilon_{\max}/2$, for the component band i .

^b Nitrobenzene was also used as solvent, but gave a spectrum insignificantly different from the chloroform solution.

^c 0.010 M in 1-cm silica cell.

^d 0.0010 M in 5-cm silica cell.

Table II

Component absorption bands of Cu(II) bis-3-ethylacetylaceton in the visible and near infrared ^a									
Solvent ^b	ω_1^0	ϵ_{1max}	$\delta_{1/2}$	ω_2^0	ϵ_{2max}	$\delta_{1/2}$	ω_s^0	ϵ_{3max}	$\delta_{1/2}$
I Chloroform ^c	19200	29	1650	15500	31	1750	--	--	--
II Acetone ^c	18700	36	1800	15600	24	1650	14300	14	2000
III 1,4-Dioxane ^c	18250	33	1650	15450	19.5	1700	14100	12.5	1900
IV Methanol ^d	17250	31	1750	15000	23	1650	13150	13.5	1750
V Pyridine	16600	44.5	1700	14650	26.5	2050	12500	16	2450

^a All frequencies and half widths given in Cm^{-1} . $\delta_{1/2}$ = half width at $\epsilon = \epsilon_{max}/2$.

^b The results with benzene as solvent were quite similar to those with chloroform.

^c 0.010 M in 1-cm silica cell.

^d 0.0040 M in 1-cm silica cell.

between the different 3d orbitals of the Cu^{++} ion perturbed by the electric field of the ligands is quite reasonable; it seems to be the only one in accordance with the observations we have just mentioned, and therefore is now shared by many workers who have recently considered transition-metal-ion visible spectra in any detail.^{1, 8, 9, 3, 4, 5, 6, 12}

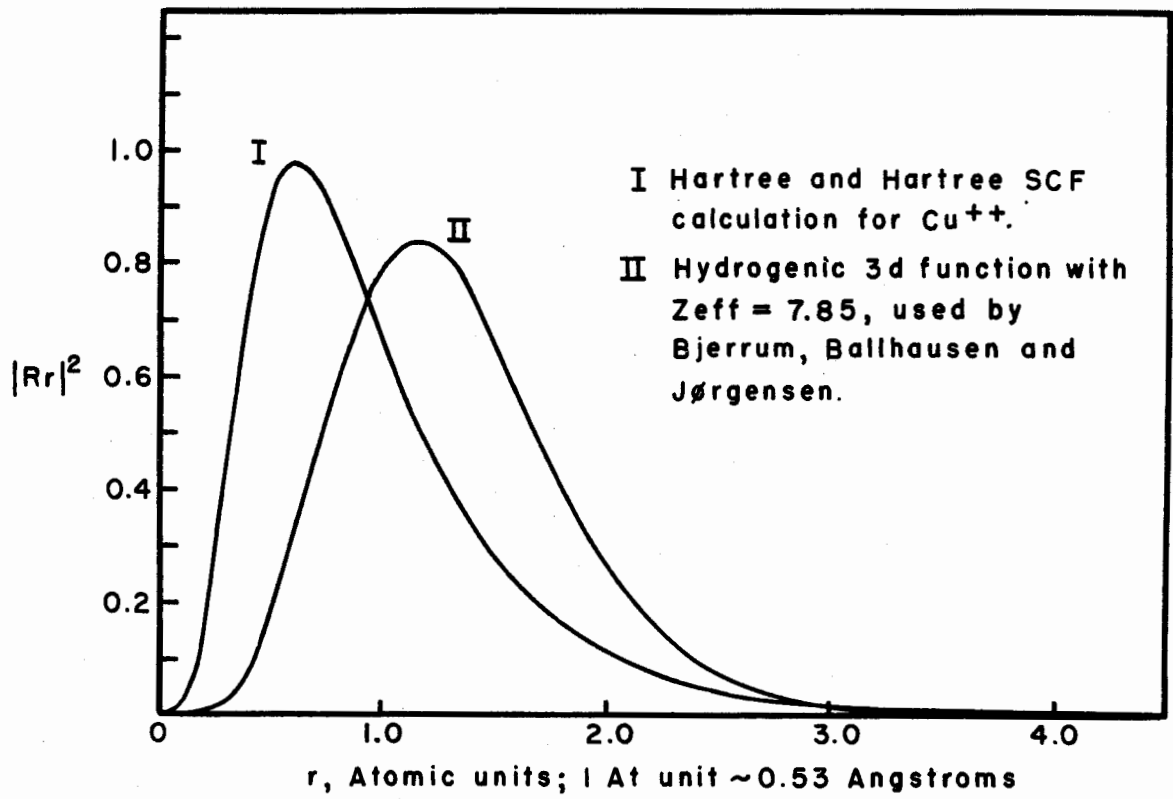
Identification of Transitions

In order to correlate the observed spectra with this theory we must examine how the Cu^{++} 3d orbital levels are split by the molecular electric field of the surrounding ligands. In Appendix I there is an account of those molecular-field (often called crystal-field) calculations which we consider pertinent to the problem at hand. We have avoided the assumption of any particular radial distribution function for the Cu^{++} 3d orbitals; although Bjerrum, Ballhausen, and Jørgensen⁸ have assumed a hydrogenlike function with seemingly good results, such a distribution must be far from the truth. The SCF (self-consistent field) calculations by Hartree and Hartree¹³ yield a 3d radial distribution function for Cu^+ . Cu^+ , obviously, is not drastically different from Cu^{++} in that respect (a point previously mentioned by Hartree and Hartree¹⁴). But this function is much at variance with the hydrogenlike function having $Z_{\text{eff}} = 7.85$ (used by the Danish workers). Both of these functions are plotted in Fig. 2. We can see that the hydrogenic function yields a maximum farther from the central ion than does the SCF function; in the environment of the ligands there might well be an orbital contraction, but expansion seems less likely. Aside from this, the loss of one electron from Cu^+ would further contract the tail of the distribution. It is instructive to plot, for both the SCF and hydrogenic function, the actual quantities, r^2 and r^4 which appear in the calculations. In this comparison, made in Fig. 3, one can see how poor an approximation the hydrogenlike function probably is. We feel that the SCF function, although not entirely satisfactory, would furnish a better basis for attempts at quantitative calculations.¹⁴ Although couched in different terms, our treatment corresponds to that by other authors.^{4, 7}

¹² Belford, Martell, and Calvin, *J. Inorg. Nucl. Chem.* 2, 11 (1956).

¹³ D. R. Hartree and W. Hartree, *Proc. Roy. Soc. (London)* 157, 490 (1936).

¹⁴ Calculations using the SCF function and avoiding the point-charge ligand model are in progress by two of us (RLB and GB).



MU-9635

Fig. 2. Comparison between self-consistent field and hydrogenic models for copper 3d radial distribution.

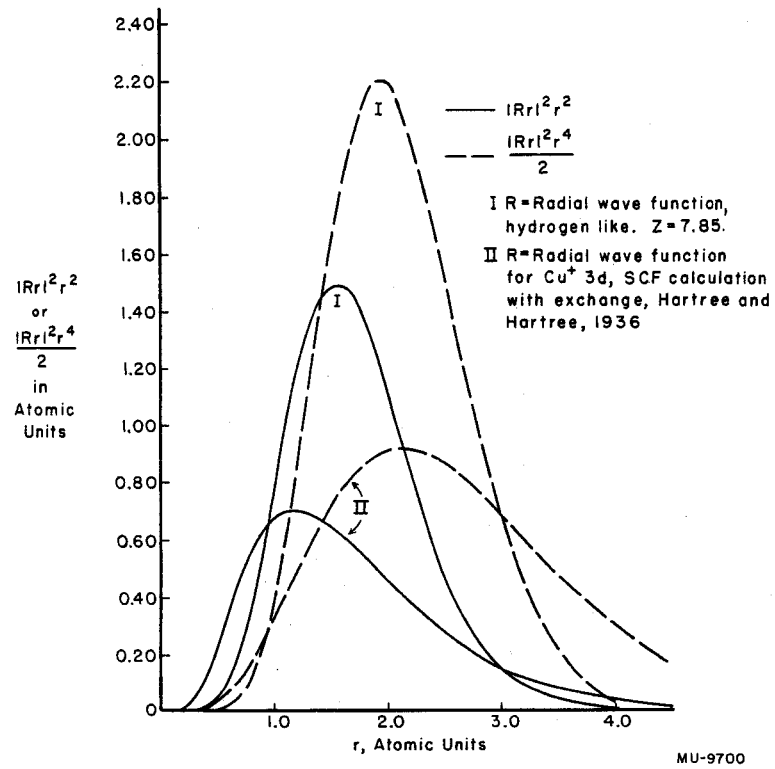


Fig. 3. Comparison of expectation values of r^2 and r^4 as derived from two copper 3d radial distributions.

To apply the crystal-field treatment to solutions of the chelate molecules at hand we must have geometrical models for them. For a noninteracting solvent, which we hope to have approached with benzene and chloroform, we need consider only isolated CuA_2 molecules. X-ray structure analysis indicates CuA_2 to be a planar molecule of D_{2h} symmetry with metal-to-oxygen distances all essentially equal.¹⁰ The dominant electrostatic field is provided by the four bound oxygen atoms, since they are copper's closest neighbors. We assume, then, that the energy levels will be but little disturbed from those given by a field of D_{4h} symmetry. The molecular field treatment in Appendix I gives the energy levels for this case as the expressions (A-14). It may be possible to further assume that for practical purposes of the calculations, the entire $3d \text{ Cu}^{++}$ electron distribution lies within a sphere and that all the charge of the ligands lies outside that sphere. Then the effect of the ligands upon the $3d$ orbital energies may be expressed in terms of point charges (whose radial coordinate and magnitude are not necessarily those of the ligand molecules). The energy levels are then described by Eq. (A-12), if only one point charge per ligand need be assumed.¹⁵

Electron transitions take place from the xz , yz orbitals to the xy ; from the $x^2 - y^2$ to the xy ; and from the $2z^2 - x^2 - y^2$ to the xy . These transitions and their energies will be called, respectively, ω_1 , ω_2 , and ω_3 . We ask whether these may be correlated with our experimental component bands in the visible and near infrared. The analysis gives three bands; so does the theory. The theoretical result predicts the following behavior for ω_1 , ω_2 , and ω_3 as two axial ligands are added to a square-planar complex to complete an axially elongated octahedron: For invariant in-plane ligand position, increasing base strength (that is, increasing effective negative charge) on the axial ligands will cause the xy and $x^2 - y^2$ levels to undergo identical shifts, will cause the xz , yz , level to approach the $x^2 - y^2$ level, and will cause the $2z^2 - x^2 - y^2$ level to approach the xy level. Thus ω_2 should remain constant but ω_1 and ω_3 decrease if one were to replace the two axial ligands in such a tetragonal hexacoordinated Cu^{++} chelate with more strongly basic ones. Furthermore, as the axial ligands approach the planar ones in basicity, ω_1 should approach ω_2 ; ω_3 should approach 0.

¹⁵ More generally, each ligand should be represented by at least two point charges at different distances from the Cu^{++} nucleus.

Now let us suppose that the solvents, which have base strengths approximately in the order previously mentioned, furnish an axial field of a strength that increases as the local base strength increases. Then to correlate an experimental band with ω_2 , we would have to find one that displays little movement from solvent to solvent. For both CuA_2 and CuEa_2 , one such does exist-- ω_{02} . Then to identify ω_1 , we would look for an experimental band lying at higher frequency than ω_{02} but approaching it as solvent basicity is increased. Again, there is one such for CuA_2 and for CuEa_2 -- ω_{01} . Finally, ω_3 would be assigned to the remaining band, provided that the remaining band decreased in frequency with increasing solvent basicity. The test is met in each case by ω_{03} . We presume, then, that $\omega_2 = \omega_{02}$, $\omega_1 = \omega_{01}$, and $\omega_3 = \omega_{03}$.

Predictions from Crystal Field Theory

Before proceeding to the consideration of effects other than crystal-field splitting we shall pause to examine the assigned bands with the assumption that the treatment should explain all the observed behavior. In so doing, we shall make some predictions and shall show that experimental results do not refute those predictions and so do not refute the premise that molecular-field splitting is a major effect in binding of our chelates.

Expressions (A-12) and (A-14) should both be useful for qualitative predictions. We see that the effect of increasing base strength (q in Eq. (A-8)) of the planar ligands should be that of increasing the over-all splitting and thus of shifting all three absorption bands to higher frequencies. For CuA_2 and CuEa_2 this prediction is borne out--all three bands of CuEa_2 are at higher frequencies than the corresponding ones of CuA_2 , as we should expect from the fact that the 3-ethyl group is an electron donor and so should increase the electron density on the four ligand oxygen atoms. A previous paper by Martell and two of us¹² illustrates the same effect for a series of five other variants upon the CuA_2 molecule, and many other examples are to be found in the literature. It is easy to see why chelate stability should be related to the position of the visible absorption bands and so to the color of the complex.¹⁶ In every case observed, the more stable chelates--those formed from the more basic ligands--produce light absorption farther toward

¹⁶ A. E. Martell and M. Calvin, *Chemistry of the Metal Chelate Compounds*, Prentice-Hall, New York, 1952.

the blue. However, since strain and other factors, not only ligand basicity, play a part in chelate stabilities, this stability criterion must be applied with discretion.

Also, the theory predicts that the ratios $\omega_1 : \omega_2 : \omega_3$ will be independent of effective ligand charge. It will be shown that such is the case for CuA_2 and CuEa_2 ; the data of Belford, Martell, and Calvin¹² seem to indicate the success of this prediction for a more varied series of ligands.

Finally, we take the values for ω_1 and ω_2 as experimental numbers and use them to calculate a predicted ω_3 (for CuA_2 in chloroform) via Eq. (A-8). The ratios of transition frequencies appear from those equations as

$$\omega_1/\omega_2 = (5/7) + (18/35) (\overline{r^2} p^2/\overline{r^4})$$

and

$$\omega_3/\omega_2 = (2/7) + (24/35) (\overline{r^2} p^2/\overline{r^4}).$$

If we take from Table I the values $\omega_1 = 18,810$ wave numbers and $\omega_2 = 15,190$ wave numbers, we find

$$\omega_1/\omega_2 = 1.24.$$

Then $(\overline{r^2} p^2/\overline{r^4}) = 1.02$. From this result we would predict an ω_3 as follows:

$$\omega_3 (\text{predicted})/\omega_2 = 0.99, \text{ or } \omega_3 (\text{pred.}) = 15,040 \text{ cm}^{-1}.$$

Thus a predicted third band would lie just under the second ($\omega_2 = 15,190 \text{ cm}^{-1}$). This very interesting result apparently agrees with experiment, for the ω_{02} for chloroform solution has an extraordinarily high intensity, a fact which suggests it to be a combination band.¹⁷ Just the same result, both calculated and observed, is obtained for CuEa_2 .

¹⁷ R. Linn Belford, Bonding and Spectra of Metal Chelates: Ultraviolet, Visible, Infrared, and Electron Resonance Absorption. Near-Infrared Spectra of Alcohols (Thesis), UCRL-3051, June 1955.

However, we regard the apparent success of numerical calculations in the previous paragraph as at least partially fortuitous. The assumptions and approximations involved are much too crude to warrant such agreement. Particularly, the value of 1.02 for $(\overline{r^2 p^2}/\overline{r^4})$ is highly artificial, since it is untenable under our assumption that the ligand and Cu^{++} 3d charge clouds do not appreciably overlap. One is forced to recognize that the ligand and metal 3d charge clouds do intermingle considerably, not only because of the anomalous value 1.02 but also because of impossibly low calculated energies for the crystal field splitting.¹⁷

Allowance for Covalency

We have seen how the molecular (crystal) field picture of Cu^{++} chelate bonding nicely explains some molecular properties. However, we note also that certain data cannot properly be interpreted on the basis of that theory alone. (This fact shows up remarkably well, according to Owen¹⁸ and McGarvey,¹⁹ in the electron-spin resonance spectra of the metal complexes.) The sizes of the electron clouds about the metal and ligand atoms are certainly great enough to cause considerable overlap, and thus exchange of electrons, among those atoms. It is reasonable to expect a considerable amount of covalent bonding in formation of the chelates. Accordingly, let us examine what covalency one may admit, in conjunction with the molecular field splitting, to obtain a better picture of bonding.

Until very recently, covalent bonding of transition metal ions in square-planar ligand environments was generally assumed to be dsp^2 . This meant that for Cu^{++} one electron must be promoted to the 4p(z) orbital, a result shown by McGarvey¹⁹ to contradict the paramagnetic resonance behavior of CuA_2 and probably likewise of CuEa_2 . Consequently, it seems worth while to use a covalent bonding scheme that is somewhat more flexible than the Pauling valence-bond ideas as they are usually applied to metal complexes. To be sure, the Pauling method is capable of reasonable results if properly applied, but we feel that the molecular orbital treatment is more suitable

¹⁸ J. Owen, Proc. Roy. Soc. (London) 227A, 183 (1955).

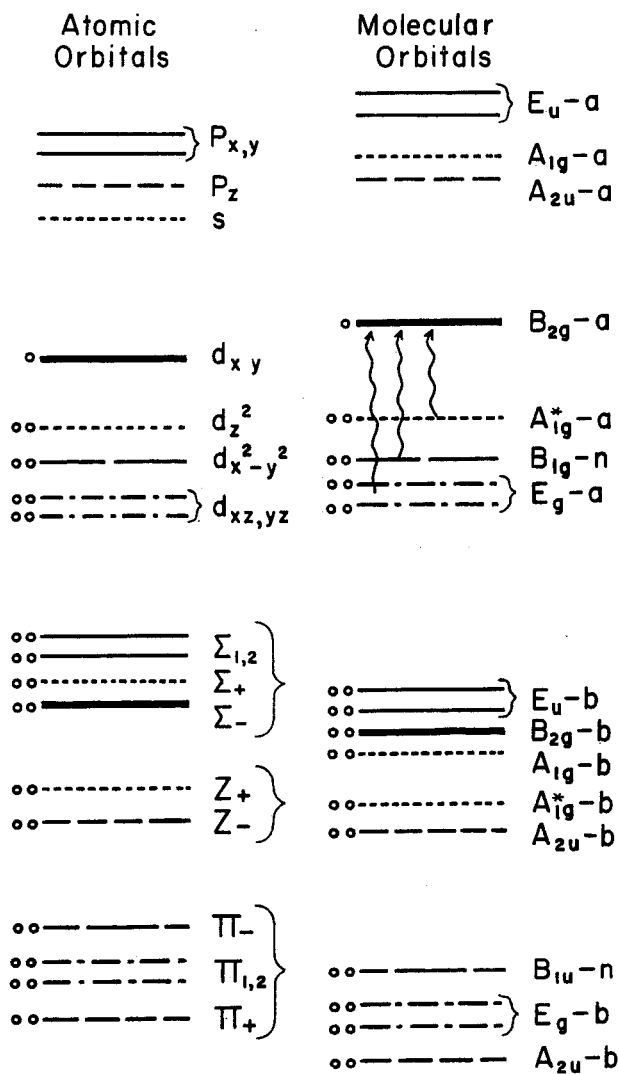
¹⁹ B. R. McGarvey, private discussion.

in this instance. Here we will consider that the molecular-field splitting has already occurred, and will simply graft to it the LCAO-MO treatment as given in Appendix II.²⁰

The scheme just described is conveniently summarized in a chart such as Fig. 4. One arrives at this kind of diagram by making rough but reasonable approximations for the parameters of the secular equations (cf. Belford¹⁷). At the left of the chart appear lines representative of energy levels (with degeneracy already broken by the ligand electric field) of the 3d, 4s, and 4p metal-ion orbitals, together with levels for ten of the ligand atomic orbitals. The "t" type have been omitted from this diagram for simplicity. On the right side are lines representing a resultant set of nineteen molecular orbital levels. Each is labeled by its group symbol together with a letter classifying it as "bonding," "antibonding," or "nonbonding," and is related to its parent atomic orbitals by means of the kind of line used. Degenerate levels are shown as separated but bracketed. The vertical direction corresponds roughly to increasing energy and is by no means quantitatively significant.

One might consider the atomic orbitals of the ligands initially filled; including copper's nine valence electrons, there are 29 electrons, which would be distributed as indicated by the open dots (Fig. 4). The unpaired electron, as shown, resides in the B_{2g} -a orbital, whose simple LCAO function is $[a d(xy) - \sqrt{1-a^2} \Sigma \dots]$. The pattern for those molecular orbitals composed principally of Cu^{++} d-orbitals may be qualitatively the same as for the d-orbitals alone. Rather a large amount of electron-exchange energy and a very great admixture of ligand atom wave functions into those d-functions might occur without a real change in the qualitative molecular field results with respect to electronic transitions. Thus the previous interpretation of the CuA_2 and CuEa_2 spectra on the basis of

²⁰ Since no accurate quantitative results can be expected from the treatment in any event, the question of which is the dominant interaction and which the perturbation upon that principal effect can be left open. For the same reason, a more elegant approach than that of Appendix II would seem profitless.



ENERGY LEVEL SCHEME IN A TETRAGONAL
Cu⁺⁺ CHELATE

MU-9378

Fig. 4. Energy-level scheme in a tetragonal Cu⁺⁺ chelate.
 o: Location of an electron.
 ~: Three postulated transitions in visible and infrared.
 } : Bracket denotes one degenerate level.
 a: "antibonding"; b: "bonding"; n: "nonbonding."

crystal field splitting need not be entirely invalidated by an appreciable amount of covalency.

Examination of the diagram shows that the so-called "dsp²" covalent bonding is obtained in cases where the B_{2g}-a level is raised above the A_{2u}-a so that the unpaired electron in its ground state resides in essentially the p(z) orbital. But clearly covalent bond energy might be quite large without that event's occurring. As a matter of fact, if pi bonding to the ligand pi system can occur, the situation is harder to reach even though covalent bonding is stronger.

MO Predictions

Our spectral data were analyzed earlier in this discussion; only ionic bonding between metal ion and ligands was considered. Now, with the aid of the MO scheme, we propose to re-examine that analysis, this time recognizing that covalent metal-to-ligand bond energies may be large -- perhaps even dominant. These last paragraphs are devoted to that inquiry.

First one must test whether our identification of transitions may be upset. Since only the solvent effect was involved in identification, we turn attention to the solvent effect of the MO scheme -- namely, the A_{1g} orbital combinations. Those ligand-solvents tending towards the stronger linkage to the metal ion would cause the greater raising of the A_{1g}*-a level and should display the smaller values for the transition A_{1g}*-a → B_{2g}-a, or ω₃. Also, possible pi-bonding orbitals of the solvent donors would have symmetry compatible with the (xz, yz) orbitals only; the combination would tend to raise E_g-a levels and so to decrease the E_g-a → B_{2g}-a transition frequency (ω₁). Moreover, no variety of solvent orbital of which we can conceive would interact noticeably with either the xy or x²-y² orbitals -- i. e., the B_{1g}-n → B_{2g}-a transition frequency (ω₂) should be nearly indifferent to solvent. Thus the solvent effects predicted from the covalent viewpoint agree with those predicted from the ionic, and our identifications remain unaltered.

Now it remains to answer the following query. When substituent groups on the CuA₂ rings are altered, do the resulting changes in copper's 3d orbital energies arise chiefly from ionic interactions, from sigma bonding, from pi bonding with π orbitals, or from pi bonding with t orbitals?

(See Appendix II.) We have shown ionic interaction (molecular field splitting) to be a plausible answer, and shall show that of the others only sigma bonding seems also acceptable.

An increase in strength of sigma bonding of the xy orbital to the oxygens' σ orbitals would raise the B_{2g} -a level, leaving the other primarily d-orbital levels unaltered. The net result would be to increase the frequency of all three transitions upon augmenting the electron-donating power of the ligand oxygens. This prediction agrees with the crystal field theory and with experiment.

On the other hand, an increase in strength of pi bonding of the ligand π system to the (xz, yz) orbitals would raise the level E_g -a, causing a decrease in ω_1 . The presumption that this interaction is dominant thus contradicts experiment (which exhibits a decrease in ω_1 as ligand donor power decreases).

Likewise, an increase in strength of t-type pi bonding of the x^2-y^2 orbital would raise the B_{1g} -n level and so require a decrease in ω_2 . This again, as a dominant effect, appears to contradict experiment.

APPENDIX

I. Molecular (Crystal) Field Treatment²¹

Here we will review briefly those calculations which describe how (a) square-planar, (b) axial, and (c) tetragonal arrangements of ligand charge around a Cu^{++} ion split the initial degeneracy of its five 3d orbitals. It is convenient to take Cu^{++} as Cu^+ plus a single 3d positron; we investigate the energy levels of the positron in the various d orbitals.

Special Case of Point-Charge Ligands

(a) First, consider Cu^{++} surrounded by four point charges arranged as in (a), Appendix II. We use the following set of 3d wave functions for Cu^{++} , expressed in polar coordinates:

$$\begin{aligned}
 d(z^2) &= R(r) \sqrt{5/16\pi} (3 \cos^2 \theta - 1), \\
 d(xz) &= R(r) \sqrt{15/4\pi} \sin \theta \cos \theta \cos \phi, \\
 d(yz) &= R(r) \sqrt{15/4\pi} \sin \theta \cos \theta \sin \phi, \\
 d(x^2 - y^2) &= R(r) \sqrt{15/16\pi} \sin^2 \theta \cos 2\phi, \\
 d(xy) &= R(r) \sqrt{15/16\pi} \sin^2 \theta \sin 2\phi,
 \end{aligned}
 \tag{A-1}$$

where $R(r)$ is the 3d radial wave function. Suppose the effect of the ligand molecular field to be addition of an extra potential energy term V to the unperturbed Hamiltonian, H_0 , of Cu^{++} . Here V is the Coulombic attraction energy between the ligand charges and the positron:

$$V = \sum_1 \frac{q_1 e^2}{r_1}, \tag{A-2}$$

where q_1 is the charge on ligand 1, and r_1 the distance from the positron to ligand 1. From the d functions we form linear variation functions ψ_i , which must satisfy the Schrödinger equations;

²¹ For extensive and detailed treatments of the calculations which we here review, see for example

- (a) H. Bethe, Ann. Phys. [5], 3, 133 (1929);
- (b) C. J. Ballhausen, loc. cit.;
- (c) H. Hartmann and F. E. Ilse, loc. cit.

$$(H_0 + V) \psi_i = (E_0 + E_i) \psi_i, \quad (i = 1, \dots, 5), \quad (\text{A-3})$$

where E_0 is the initial 3d level, taken for convenience as the zero point of energy, and E_i the extra energy produced by V . The E_i are solutions of the secular equation

$$\left| \int V d_j d_l d\tau - \delta_{lj} E \right| = 0. \quad (\text{A-4})$$

One can easily verify that for a V of C_4 symmetry this secular determinant is diagonal, so that we have

$$E_k = \int_0^\infty \int_0^\pi \int_0^{2\pi} \frac{2}{d_i} V r^2 \sin \theta d\phi d\theta dr. \quad (\text{A-5})$$

Now, in order to evaluate these integrals, we expand both V and the $\frac{2}{d_k}$ in a series of orthonormal functions, the normalized surface harmonics, $L_n^m(\theta, \phi)$. Those which are used here are listed in Table III.

The $\frac{2}{d_k}$ become

$$\begin{aligned} \frac{2}{d(z^2)} &= \left[1/4 \pi + (\sqrt{5}/7 \sqrt{\pi}) L_2^0 + (3/7 \sqrt{\pi}) L_4^0 \right] R^2, \\ \frac{2}{d(xz)} &= \left[1/4 \pi + (\sqrt{5}/14 \sqrt{\pi}) L_2^0 + (\sqrt{15}/14 \sqrt{\pi}) L_2^2 \right. \\ &\quad \left. - (2/7 \sqrt{\pi}) L_4^0 - (\sqrt{5}/7 \sqrt{\pi}) L_4^2 \right] R^2, \\ \frac{2}{d(yz)} &= \left[1/4 \pi + (\sqrt{5}/14 \sqrt{\pi}) L_2^0 + (\sqrt{15}/14 \sqrt{\pi}) L_2^2 \right. \\ &\quad \left. - (2/7 \sqrt{\pi}) L_4^0 + (\sqrt{5}/7 \sqrt{\pi}) L_4^2 \right] R^2, \\ \frac{2}{d(x^2 - y^2)} &= \left[1/4 \pi - (\sqrt{5}/7 \sqrt{\pi}) L_2^0 + (1/14 \sqrt{\pi}) L_4^0 \right. \\ &\quad \left. + (\sqrt{35}/14 \sqrt{\pi}) L_4^4 \right] R^2, \\ \frac{2}{d(xy)} &= \left[1/4 \pi - (\sqrt{5}/7 \sqrt{\pi}) L_2^0 + (1/14 \sqrt{\pi}) L_4^0 \right. \\ &\quad \left. - (\sqrt{35}/14 \sqrt{\pi}) L_4^4 \right] R^2; \end{aligned} \quad (\text{A-6})$$

Table III

Normalized Surface Harmonics		
n	m	L_n^m
0	0	$1/\sqrt{4\pi}$
2	0	$\sqrt{5/16\pi} (3 \cos^2 \theta - 1)$
2	2	$\sqrt{15/16\pi} \sin^2 \theta \sin 2\phi$
4	0	$3/16\sqrt{\pi} (3 - 30 \cos^2 \theta + 35 \cos^4 \theta)$
4	2	$\sqrt{45/64\pi} \sin \theta (1 - 7 \cos^2 \theta) \cos 2\phi$
4	4	$\sqrt{315/256\pi} \sin^2 \theta \cos 4\phi$

and (A-2) may be written as

$$V(\text{sq.}) = \frac{4q_1 e^2}{P} \left[1 - \sqrt{\pi/5} (r/P)^2 L_2^0 + \sqrt{\pi/16} (r/P)^4 L_4^0 - (\sqrt{35\pi/12} (r/P)^4 L_4^4 + \dots) \right], \quad (\text{A-7})$$

where P is the distance from a ligand charge to the Cu^{++} nucleus. The orthonormal property of the L 's gives us immediately

$$\begin{aligned} E(z^2)_{\text{sq.}} &= + \frac{4q_1 e^2}{P} \left(1 - \frac{1}{7} \frac{\overline{r^2}}{p^2} + \frac{3}{28} \frac{\overline{r^4}}{p^4} \right), \\ E(xz)_{\text{sq.}} &= E(yz)_{\text{sq.}} = + \frac{4q_1 e^2}{P} \left(1 - \frac{1}{14} \frac{\overline{r^2}}{p^2} - \frac{1}{14} \frac{\overline{r^4}}{p^4} \right), \\ E(x^2 - y^2)_{\text{sq.}} &= + \frac{4q_1 e^2}{P} \left(1 + \frac{1}{7} \frac{\overline{r^2}}{p^2} - \frac{4}{21} \frac{\overline{r^4}}{p^4} \right), \quad \text{and} \\ E(xy)_{\text{sq.}} &= + \frac{4q_1 e^2}{P} \left(1 + \frac{1}{7} \frac{\overline{r^2}}{p^2} + \frac{19}{84} \frac{\overline{r^4}}{p^4} \right); \end{aligned} \quad (\text{A-8})$$

where $\overline{r^n}$ is the expectation value of r^n :

$$\overline{r^n} = \int_0^{\infty} R^2 r^{n+2} dr. \quad (\text{A-9})$$

(b) Next, consider the effect of two charges, q_z , along the z axis; their positions are $(0, 0, z')$, $(0, 0, -z')$. The work is exactly the same as in (a). Here the potential term is

$$V_{\text{axial}} = \frac{2q_z e^2}{z'} = \left[1 + \sqrt{4\pi/5} (r z')^2 L_2^0 + \sqrt{4\pi/9} (r z')^4 L_4^0 + \dots \right]. \quad (\text{A-10})$$

The contribution to energy level of the axial charges is then

$$E(z^2)_{\text{axial}} = \frac{2q_z e^2}{z'} \left(1 + \frac{2}{7} \frac{\overline{r^2}}{z'^2} + \frac{2}{7} \frac{\overline{r^4}}{z'^4} \right),$$

$$E(yz)_{\text{axial}} = E(xz)_{\text{axial}} = \frac{2q_z e^2}{z'} \left(1 + \frac{1}{7} \frac{\overline{r^2}}{z'^2} - \frac{4}{21} \frac{\overline{r^4}}{z'^4} \right), \quad (\text{A-11})$$

$$E(x^2 - y^2)_{\text{axial}} = E(xy)_{\text{axial}} = \frac{2q_z e^2}{z'} \left(1 - \frac{2}{7} \frac{\overline{r^2}}{z'^2} + \frac{1}{21} \frac{\overline{r^4}}{z'^4} \right).$$

(c) Next, we can compute the effect of a tetragonal (including the special case of cubic) arrangement of ligand charge by adding corresponding quantities in Eqs. (A-8) and (A-11). Thus we have

$$E(K)_{\text{tetragonal}} = E(k)_{\text{sq.}} + E(k)_{\text{axial}}. \quad (\text{A-12})$$

Figure 5 pictures the results of (a), (b), and (c).

General Case

Suppose we lift the restriction that the ligands be approximated by point charges and assume for them a continuous charge density with D_{4h} symmetry; the symmetry of ligand nuclei about the central ion is sufficient to determine the charge-density symmetry. Then consider an infinitesimally thin spherical shell of thickness dy and radius γ , centered at the Cu^{++}

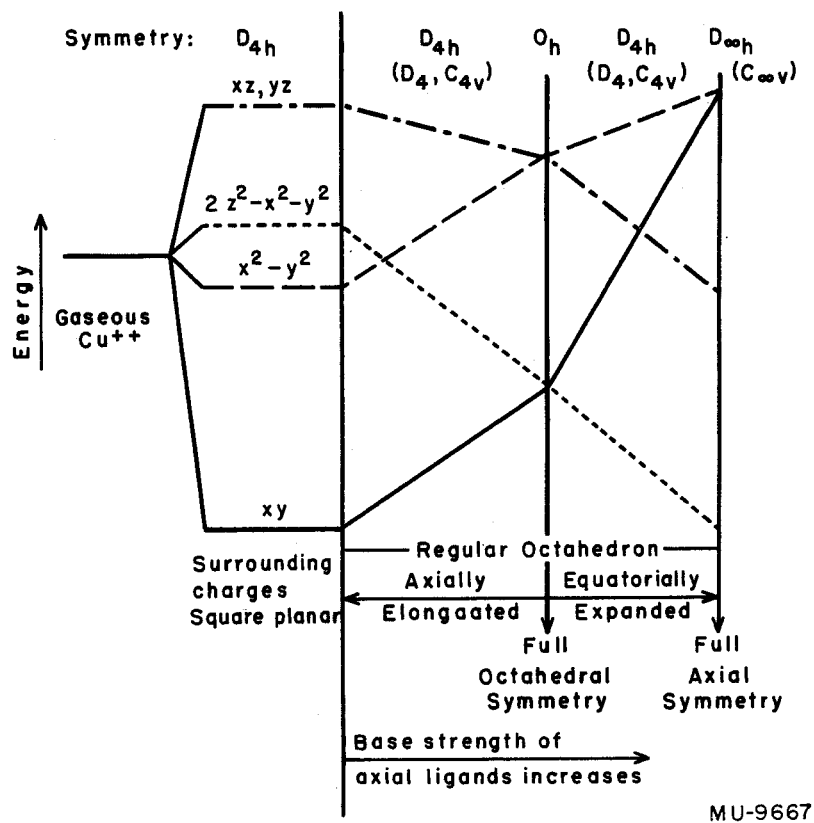


Fig. 5. Schematic representation of positron energy levels of cupric ion in crystal or molecular fields of various strengths and symmetries.

nucleus and containing ligand charge. Then the first terms in the expansion of the potential V are given by

$$\begin{aligned} dV_{\gamma} = & \left[A_0(\gamma) d\gamma + A_0'(\gamma)/r \right] d\gamma + L_2^0 \left\{ \left[A_2(\gamma) r^2 \right]_{r < \gamma} \right. \\ & \left. + \left[A_2'(\gamma)/r^3 \right]_{r > \gamma} \right\} d\gamma + L_4^0 \left\{ \left[A_4(\gamma) r^4 \right]_{r < \gamma} + \left[A_4'(\gamma)/r^5 \right]_{r > \gamma} \right\} d\gamma \\ & + L_4^4 \left\{ \left[A_{sq}(\gamma) r^4 \right]_{r < \gamma} + \left[A_{sq}'(\gamma)/r^5 \right]_{r > \gamma} \right\} d\gamma. \end{aligned} \quad (A-13)$$

The coefficients $A_{sq}(\gamma)$ have no contributions from an axially symmetric charge cloud--that is, effectively, from the two axially situated ligands. Now, integration is carried out over γ . Multiply Eq. (A-13) by the (A-6) and integrate over r, ϕ, θ as before, and then over γ to include all the ligand charge, to obtain

$$\begin{aligned} E(z^2)_{tet} &= A_0 + 2\sqrt{5} A_2 + 6A_4, \\ E(yz)_{tet} = E(xz)_{tet} &= A_0 + \sqrt{5} A_2 - 4A_4, \\ E(x^2 - y^2)_{tet} &= A_0 - 2\sqrt{5} A_2 + A_4 + \sqrt{35} A_{sq}, \\ E(xy)_{tet} &= A_0 - 2\sqrt{5} A_2 + A_4 - \sqrt{35} A_{sq}, \end{aligned} \quad (A-14)$$

where

$$A_0 = \int_0^{\infty} \left[\int_0^{\gamma} A_0(\gamma) r^2 R^2 dr + \int_{\gamma}^{\infty} A_0'(\gamma) r R^2 dr \right] d\gamma, \quad (A-15)$$

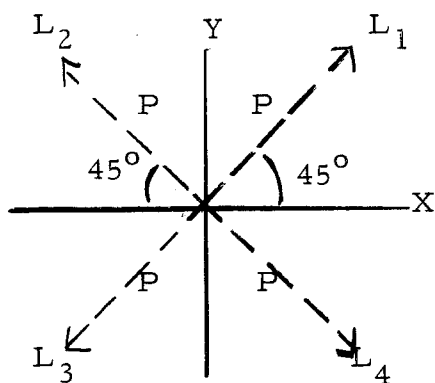
$$A_i \neq_0 = (1/14\sqrt{\pi}) \int_0^{\infty} \left[\int_0^{\gamma} A_i(\gamma) r^{n+2} R^2 dr + \int_{\gamma}^{\infty} A_i'(\gamma) r^{1-n} R^2 dr \right] d\gamma$$

$$(n = 2 \text{ for } i = 2; 4 \text{ for } i = 4, sq). \quad (A-16)$$

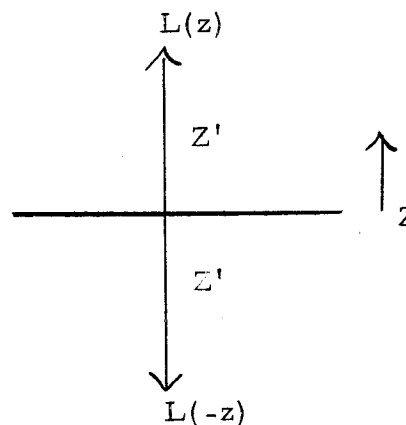
II: Molecular Orbital Treatment

This section contains an account of a simple molecular orbital scheme for the binding of copper complexes. We consider a Cu^{++} ion with the following set of nine orbitals that might be available for bonding: $d(xy)$, $d(x^2-y^2)$, $d(xz)$, $d(yz)$, $d(z^2)$, s , $p(x)$, $p(y)$, and $p(z)$.

Now we take a set of fourteen orbitals, which might be furnished by six surrounding ligands placed as shown in (A) and (B):



(A)



(B)

The Cu nucleus is here taken as the center of the coordinate system. Twelve of the ligand orbitals would arise from L_1 , L_2 , L_3 , and L_4 thus; for each, there would be an orbital, called σ_1 , σ_2 , σ_3 , and σ_4 , directed along the internuclear axis (45° line); two p-type orbitals directed perpendicular to the 45° line--one, called t_1, t_2, t_3 or t_4 , having a nodal plane perpendicular to the x, y plane, and the other, called π_1, π_2, π_3 , or π_4 , having the x, y plane as node. The remaining two ligands, $L(z)$ and $L(-z)$, are presumed to have orbitals, named $\sigma(z)$ and $\sigma(-z)$, directed along the z axis toward the Cu nucleus.

Now we make use of an assumed symmetry for the complex: D_{4h} . By means of group theory we can factor the secular determinant containing all orbitals we have mentioned into blocks, each of which is denoted as usual by the customary symbol for the irreducible representation Γ_i to which its n_i orbitals $\phi(\Gamma_i)$ belong. The Γ_i and $\phi(\Gamma_i)$ are shown in Table IV.

Table IV

Reduction of the 23-dimensional representation into irreducible blocks, with new basis functions

\prod_i	$\phi(\prod_i)$	Secular Determinant for \prod_i			
A_{1g}	$\sum_+ \equiv \frac{1}{2} [\sigma_1 + \sigma_2 + \sigma_3 + \sigma_4]$	$Q_s - W$	$2\beta_s, \sigma_1$	0	$\sqrt{2}\beta_s, \sigma(z)$
	s	$2\beta_s, \sigma_1$	$Q_{\sigma_1}^{-W}$	$2\beta_{d(z)^2}, \sigma_1$	0
	$d(z)^2$	0	$2\beta_{d(z)^2}, \sigma_1$	$Q_{d(z)^2}^{-W}$	$\sqrt{2}\beta_{d(z)^2}, \sigma(z)$
	$Z_+ \equiv \frac{1}{\sqrt{2}} [\sigma(z) + \sigma(-z)]$	$\sqrt{2}\beta_s, \sigma(z)$	0	$\sqrt{2}\beta_{d(z)^2}, \sigma(z)$	$Q_{\sigma(z)}^{-W}$
A_{2g}	$T_+ \equiv \frac{1}{2} [t_1 + t_2 + t_3 + t_4]$	$Q_{t_1}^{-W}$			
A_{2u}	$\pi_+ \equiv \frac{1}{2} [\pi_1 + \pi_2 + \pi_3 + \pi_4]$	$Q_{p(z)}^{-W}$	$2\beta_{p(z)}, \pi_1$	$\sqrt{2}\beta_{p(z)}, \sigma(z)$	
	$Z_- \equiv \frac{1}{\sqrt{2}} [\sigma(z) - \sigma(-z)]$	$2\beta_{p(z)}, \pi_1$	$Q_{\pi_1}^{-W}$	0	
	$p(z)$	$\sqrt{2}\beta_{p(z)}, \sigma(z)$	0	$Q_{\sigma(z)}^{-W}$	

Table IV (continued)

Γ_i	$\phi(\Gamma_i)$	Secular Determinant for Γ_i
B_{1g}	$d(x^2 - y^2)$	$Q_{d(x^2 - y^2)} - W$
	$T_- = \frac{1}{2} [t_1 - t_2 + t_3 - t_4]$	$2 \beta_{d(x^2 - y^2), t_1} Q_{t_1} - W$
B_{1u}	$\pi_- = \frac{1}{2} [\pi_1 - \pi_2 + \pi_3 - \pi_4]$	$Q_{\pi_1} - W$
B_{2g}	$d(xy)$	$Q_{d(xy)} - W$
	$\sum_- = \frac{1}{2} [\sigma_1 - \sigma_2 + \sigma_3 - \sigma_4]$	$2 \beta_{d(xy), \sigma_1} Q_{\sigma_1} - W$
E_g	$d(xz)$	$Q_{d(yz)} - W$
	$\pi_1 = \frac{1}{2} [\pi_1 - \pi_2 - \pi_3 + \pi_4]$	$2 \beta_{d(yz), \pi_1} Q_{\pi_1} - W$
	degenerate with	
	$d(yz)$	
	$\pi_2 = \frac{1}{2} [\pi_1 + \pi_2 - \pi_3 - \pi_4]$	

2

Table IV (continued)

Γ_i	$\phi(\Gamma_i)$	Secular Determinant for Γ_i	2
E_u	$\sum_1 \equiv \begin{cases} p(x) \\ \sigma_1^3 - \sigma_2 - \sigma_3 + \sigma_4 \end{cases}$	$Q_{p(y)-W}$	$2 \beta_{p(y), t_1}$
	$T_1 \equiv \frac{1}{2} [t_1 + t_2 - t_3 - t_4]$	Q_{σ_1-W}	0
B_{1u}	degenerate with		
	$\sum_2 \equiv \begin{cases} p(y) \\ \sigma_1 + \sigma_2 - \sigma_3 - \sigma_4 \end{cases}$	0	Q_{t_1-W}
	$T_2 \equiv \frac{1}{2} [-t_1 + t_2 + t_3 - t_4]$	Q_{π_1-W}	
B_{2g}	$d(xy)$	$Q_{d(xy)-W}$	$2 \beta_{d(xy), \sigma_1}$
	$\sum_- \equiv \frac{1}{2} [\sigma_1 - \sigma_2 + \sigma_3 - \sigma_4]$	$2 \beta_{d(xy), \sigma_1}$	Q_{σ_1-W}

Table IV (continued)

Γ_i	$\phi(\Gamma_i)$	Secular Determinant for Γ_i
E_g	$d(xy)$	$Q_{d(yz)}^{-W}$
	$\pi_1 \equiv \frac{1}{2} [\pi_1 - \pi_2 - \pi_3 + \pi_4]$	$2 \beta_{d(yz), \pi_1}^2$
	degenerate with	
	$d(yz)$	
E_u	$\pi_2 \equiv \frac{1}{2} [\pi_1 + \pi_2 - \pi_3 - \pi_4]$	$Q_{\pi_1}^{-W}$
	$p(x)$	$Q_{p(y)}^{-W}$
	$\sum_1 \equiv \frac{1}{2} [\sigma_1 + \sigma_2 - \sigma_3 + \sigma_4]$	$2 \beta_{p(y), \sigma_1}^2$
	$T_1 \equiv \frac{1}{2} [t_1 + t_2 - t_3 - t_4]$	$2 \beta_{p(y), t_1}^2$
	degenerate with	
E_u	$p(y)$	$Q_{\sigma_1}^{-W}$
	$\sum_2 \equiv \frac{1}{2} [\sigma_1 + \sigma_2 - \sigma_3 - \sigma_4]$	0
	$T_2 \equiv \frac{1}{2} [-t_1 + t_2 + t_3 - t_4]$	0
		$Q_{t_1}^{-W}$

Symbols for the usual LCAO-MO integrals are defined as follows:

$$Q_{\phi_r} = \int \overline{\phi_r} H \phi_r d\tau, \text{ the "Coulomb integral,"}$$

$$\beta_{\phi_r \phi_j} = \int \overline{\phi_r} H \phi_j d\tau, \text{ the "exchange integral,"}$$

where H is the Hamiltonian for the problem. If the true wave functions $\psi(\Gamma_i)$ are assumed to be linear variation functions of the $\phi(\Gamma_i)$, we have

$$\psi_k(\Gamma_i) = \sum_{r=1}^{n_i} a_{kr} \phi_r(\Gamma_i);$$

then if we (a) consider the ϕ_r as an orthonormal set, (b) neglect overlap (except as it is corrected for in the choice of Coulomb and exchange integrals) and all direct interligand exchange and all other perturbations, (c) set $\beta_{rj} = \beta_{jr}$, and (d) take account of the equivalence of $L_1 \dots L_4$, of $L(z)$ and $L(-z)$, of $p(x)$ and $p(y)$, and of $d(xz)$ and $d(yz)$, the energy levels for our simple system are the solutions W to the secular equations, which are also listed in Table IV.

This work was done under the auspices of the U. S. Atomic Energy Commission.